

Award Number: W81XWH-13-1-0050

TITLE: Development of Ultrasound to Measure In-vivo Dynamic Cervical Spine Intervertebral Disc Mechanics

PRINCIPAL INVESTIGATOR: Brian Snyder

CONTRACTING ORGANIZATION: Beth Israel Deaconess Medical Center
Boston, MA 02215

REPORT DATE: January 2016

TYPE OF REPORT: Annual Report

PREPARED FOR: U.S. Army Medical Research and Materiel Command
Fort Detrick, Maryland 21702-5012

DISTRIBUTION STATEMENT: Approved for Public Release; Distribution Unlimited

The views, opinions and/or findings contained in this report are those of the author(s) and should not be construed as an official Department of the Army position, policy or decision unless so designated by other documentation.

REPORT DOCUMENTATION PAGE			<i>Form Approved</i> OMB No. 0704-0188		
Public reporting burden for this collection of information is estimated to average 1 hour per response, including the time for reviewing instructions, searching existing data sources, gathering and maintaining the data needed, and completing and reviewing this collection of information. Send comments regarding this burden estimate or any other aspect of this collection of information, including suggestions for reducing this burden to Department of Defense, Washington Headquarters Services, Directorate for Information Operations and Reports (0704-0188), 1215 Jefferson Davis Highway, Suite 1204, Arlington, VA 22202-4302. Respondents should be aware that notwithstanding any other provision of law, no person shall be subject to any penalty for failing to comply with a collection of information if it does not display a currently valid OMB control number. PLEASE DO NOT RETURN YOUR FORM TO THE ABOVE ADDRESS.					
1. REPORT DATE January 2016		2. REPORT TYPE Annual		3. DATES COVERED 27DEC2014 - 26DEC2015	
4. TITLE AND SUBTITLE Development of Ultrasound to Measure In-vivo Dynamic Cervical Spine Intervertebral Disc Mechanics			5a. CONTRACT NUMBER W81XWH-13-1-0050		
			5b. GRANT NUMBER		
			5c. PROGRAM ELEMENT NUMBER		
6. AUTHOR(S) Brian Snyder E-Mail: Brian.Snyder@childrens.harvard.edu			5d. PROJECT NUMBER		
			5e. TASK NUMBER		
			5f. WORK UNIT NUMBER		
7. PERFORMING ORGANIZATION NAME(S) AND ADDRESS(ES) Beth Israel Deaconess Medical Center 330 Brookline Avenue, Boston, MA Medical College of Wisconsin 8701 W Watertown Plank Rd, Milwaukee, WI 53226			8. PERFORMING ORGANIZATION REPORT		
9. SPONSORING / MONITORING AGENCY NAME(S) AND ADDRESS(ES) U.S. Army Medical Research and Materiel Command Fort Detrick, Maryland 21702-5012			10. SPONSOR/MONITOR'S ACRONYM(S)		
			11. SPONSOR/MONITOR'S REPORT NUMBER(S)		
12. DISTRIBUTION / AVAILABILITY STATEMENT Approved for Public Release; Distribution Unlimited					
13. SUPPLEMENTARY NOTES					
14. ABSTRACT We developed a unique dual ultrasound system that can non-invasively measure Intervertebral Disc (IVD) deformation and mechanical compliance ex-vivo and in-vivo. The system is capable of providing real-time images of IVDs and dynamic vertebral motion during simulated tasks. Vertebrae motion and IVD deformation were measured by tracking the bony surface profiles in consecutive US images. Classical Voigt model and finite element model were built to investigate the "transfer function" human cadaveric spine functional spine units to account for the differential elasticity during compression or tension. As a portable, low cost imaging modality, the dual ultrasound system quantified cervical spine IVD displacement and the mechanical compliance of a functional spinal unit (FSU) in response to applied forces. This technology allowed in-vivo evaluation of cervical spine mechanical behavior in dynamic environments where MRI and CT cannot be used..					
15. SUBJECT TERMS Nothing listed					
16. SECURITY CLASSIFICATION OF:			17. LIMITATION OF ABSTRACT	18. NUMBER OF PAGES	19a. NAME OF RESPONSIBLE PERSON USAMRMC
a. REPORT U	b. ABSTRACT U	c. THIS PAGE U			19b. TELEPHONE NUMBER (include area code)
			UU	27	

Contents

1. ABSTRACT	4
2. INTRODUCTION	4
3. PROGRESS	5
3.1 Cervical Design and Production	5
3.2 <i>In-vivo</i> Dual US Test in Repetitive Jumps.....	6
3.3 In-vivo US Test in Sim Environment	9
3.4 Fatigue Experiments on Cervical Spine Disc Segments and Developing a FE Product to Predict Spine Fatigue Using the Experimental Data.....	12
3.4.1 Experiments.....	12
3.4.2 Finite Element Modeling.....	17
4. CONCLUSION	24
5. REPORTABLE OUTCOMES	24
5.1 Conference Presentation	24
5.2 Publication	25
6. REFERENCE	26

1. ABSTRACT

We developed a unique dual ultrasound system that can non-invasively measure Intervertebral Disc (IVD) deformation and mechanical compliance *ex-vivo* and *in-vivo*. The system is capable of providing real-time images of IVDs and dynamic vertebral motion during simulated tasks. Vertebrae motion and IVD deformation were measured by tracking the bony surface profiles in consecutive US images. Classical Voigt model and finite element model were built to investigate the “transfer function” human cadaveric spine functional spine units to account for the differential elasticity during compression or tension. As a portable, low cost imaging modality, the dual ultrasound system quantified cervical spine IVD displacement and the mechanical compliance of a functional spinal unit (FSU) in response to applied forces. This technology allowed *in-vivo* evaluation of cervical spine mechanical behavior in dynamic environments where MRI and CT cannot be used.

2. INTRODUCTION

Neck pain is pervasive problems in military population, especially in those working in vibrating environments. Previous studies show neck pain is strongly associated with degeneration of Intervertebral Disc (IVD), which is commonly caused by repetitive loading and aging. To reduce the risk of cervical spine disease, there is a need to measure the effect by helmet, equipment and seating. However, *in-vivo* displacement and loading condition of cervical spine are difficult to measure during operation. Clinical ultrasound (US) is being explored as a tool to image motion of the cervical spine, specifically vertebral kinematics and IVD deformation. A dual US imaging system is being developed to measure 3D motion of contiguous cervical vertebrae and IVD strain (Δ height of IVD/original IVD height) of intervening functional spine units (FSU). This system was validated *ex-vivo* using cadaveric C-spines mounted in a servo-hydraulic material testing machine by comparing dynamic US measurement to direct measurements using the linear variable differential transformer (LVDT) of the hydraulic test system.

Over the past year of support, 2015-2016, we finalized the protocol of applying dual US on human subjects performing simulated tasks, ex. jump test and cyclic loading test. The capability of the dual US to measure C-spine elastic and viscoelastic properties *in-vivo* under conditions simulating vibrations over a range of frequencies and amplitudes is currently being studied. Preliminary tests result suggested that para-cervical muscles are capable of stiffening the FSUs and minimizing the magnitude of IVD deformation. Finite element (FE) models of the IVD were developed to examine the disc injury mechanism in response to repetitive loading forces and moments applied to the head and neck.

3. PROGRESS

3.1 Cervical Design and Production

In-vivo FSU deformation measurement by Dual US was challenging without a proper design of cervical collar over the years. As a planar imaging method, US required relatively fixed imaging windows and angles during the examination. In our previous *ex-vivo* validation experiments, the overall mean absolute error of US measurements was 0.041 mm for applied frequencies 1-8 Hz. Assuming typical IVD deformation of 0.8mm under 150N load, this corresponds to a 6.3% precision error in the US measured strain. However, the large range of neck motion brought issues of stabilizing ultrasound transducer on human volunteer during *in-vivo* experiments: on one hand, loose contact between transducer and neck skin caused miss of vertebrae image, and affected accuracy of FSU deformation measurement; on the other hand, using devices such as orthotic collar guaranteed quality of dual US imaging, but the range of neck motion was limited.

A flexible neoprene fabric cervical collar (Figure 1 **Error! Reference source not found.**) was developed to mount ultrasound probes in effort to provide reliable US measurement of *in-vivo* FSU deformation on volunteers in activities (ex. jumping or cyclic neck compression/tension). Tensive adhesive gel (Parker Laboratories, Fairfield, NJ) maintained probe-to-skin contact over the testing period. In current study protocol, human subjects perform 6 trials of 4-minutes jumping with a motorcycle helmet. Subjects were able to extend and flex neck with the ultrasound devices and helmet mounted. Compared to previous collars, US imaging generally maintained equivalent quality as the trials with a rigid orthotic collar, which only provides flexibility to neck motion in superior-inferior direction.

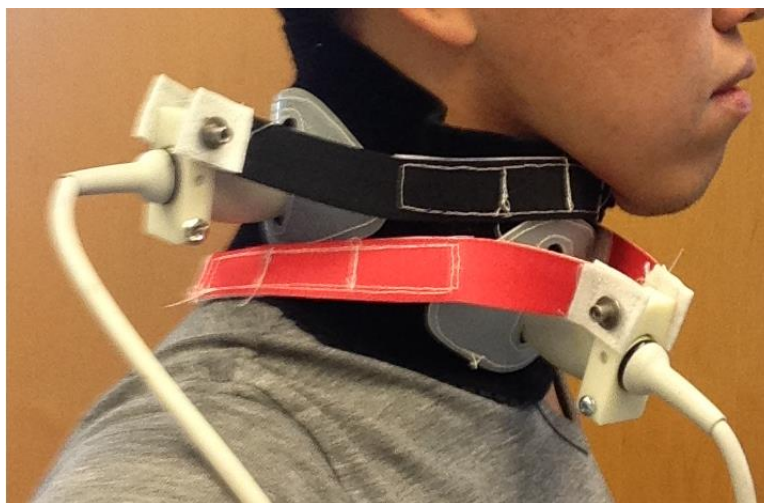


Figure 1 The flexible neck-seal collar has two openings for the insertion of ultrasound probes to image vertebral bodies anteriorly and laminae posteriorly. On the outer surface, fabric strip provides mating sites for other fabric strips. Ultrasound probe was fastened on its tail end by multiple elastic bands. The flexibility of neoprene allows subject to perform jumping, flexion/extension in certain degree without loss of ultrasound images.

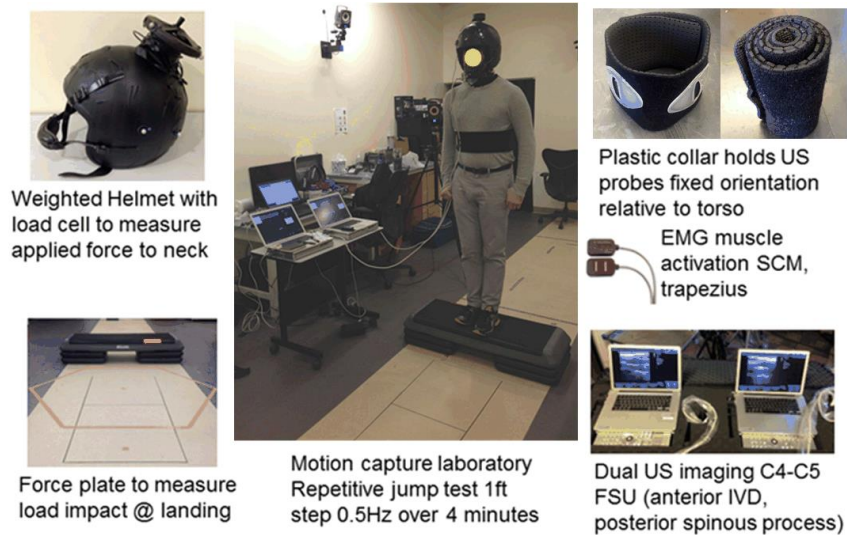


Figure 2. Human volunteer performing repetitive jumping task with a geared helmet. Impact to head and impact during landing were measured by load cell and force plate. The resultant C4-C5 FSU deformation was imaged by dual ultrasound system during jumping. Para-cervical muscles (SCM, upper trapezius) activation were measured by non-invasive surface EMG.

3.2 *In-vivo* Dual US Test in Repetitive Jumps

The aim of study is to measure the effect of para-spinal muscle activation of deformation of FSU/IVD during repetitive jumping (simulated tasks) by using dual US system. 8 human subjects were recruited under IRB approval by Committee on Clinical Investigation at BIDMC. We hypothesized reflexive contraction of the para-cervical muscles helped to dampen the extra force transmitted to the cervical spine, but prolonged and recurrent jumping may result in muscle fatigue with increased load applied to the IVD and a change of dynamic compliance of the FSU/IVD. IVD integrity was evaluated in T₂-weighted Magnetic Resonance(MR) Images for all subjects in BIDMC Radiology. Subject repetitively jumped on/off 0.8 feet step at 0.5Hz landing with both feet on force plate while maintaining upright posture for 4 minutes, wearing a helmet to simulate military head gear (Figure 2).

The motorcycle helmet subject wore during jump activities weighted 4 lbs. with additional 2.5 weight to mimic night vision goggle and communication unit. 7 passive reflective optical markers were placed on the helmet and torso to track relative displacements of head relative to the first thoracic vertebrae by Vicon Motion Capture System (10 MX-T40 cameras, Vicon Industries Inc., Hauppauge, NY). C4-C5 FSU superior-inferior deformation was measured by dual US (2 Terason t3200 systems synchronized to collaboratively capture US image, Terason, Burlington, MA) with 15L4 linear arrays (frequency 4-15 MHz). A surface electromyograms (sEMG) system (Delsys® Bagnoli) was used to evaluate para-cervical muscle activities by collecting sEMG of upper Trapezius and Sternocleidomastoid muscles. The compressive applied load by extra weight and landing force profile were measured by a miniature load cell (iLoad Mini, Loadstar Sensors, Fremont, CA) embedded in helmet and a grounded force plate (Figure 3).

The number of times that EMG signal exceeded a set threshold (0.1V/1k amp & 1V/10k amp for upper Trapezius and SCM respectively) were used to evaluate the intensity of EMG activation times in a period. The para-cervical muscle activities were compared between volunteers who have regular strength training vs. endurance training. Volunteer who participates in weight training program has greater muscle activation signal, compared the volunteer who does swimming (endurance training, Figure 4 A/B vs. D/E). However, fatigue became apparent sooner in the weight training volunteer (activities decreasing over time, slope = -0.17 s^{-1}) compared to endurance training volunteer (activities remaining relatively constant, slope = -0.012 s^{-1} , Figure 4 Error! Reference source not found. C vs. F).

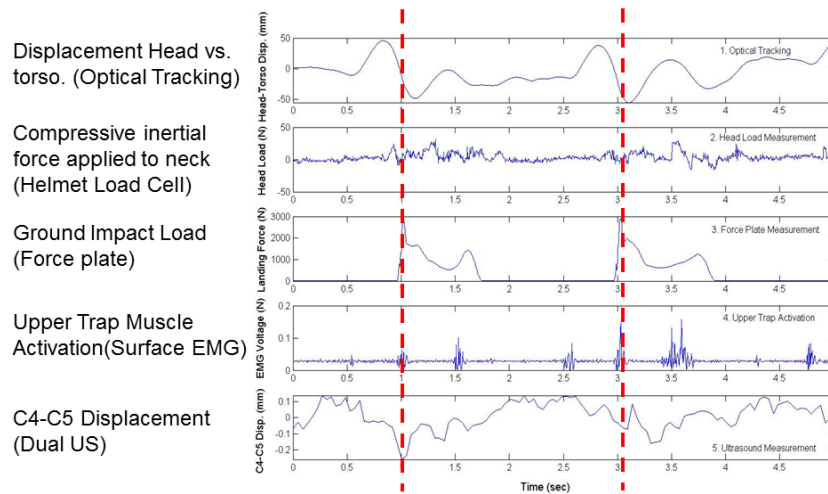


Figure 3. Synchronized measurements over 5 seconds (2 jumps) with un-weighted helmet. Impact force profile during landing @ time that load measured by force plate reached its maximum synchronized with IVD deformation measured by dual US and para-cervical muscle activation measured by EMG (marked by red dashed line).

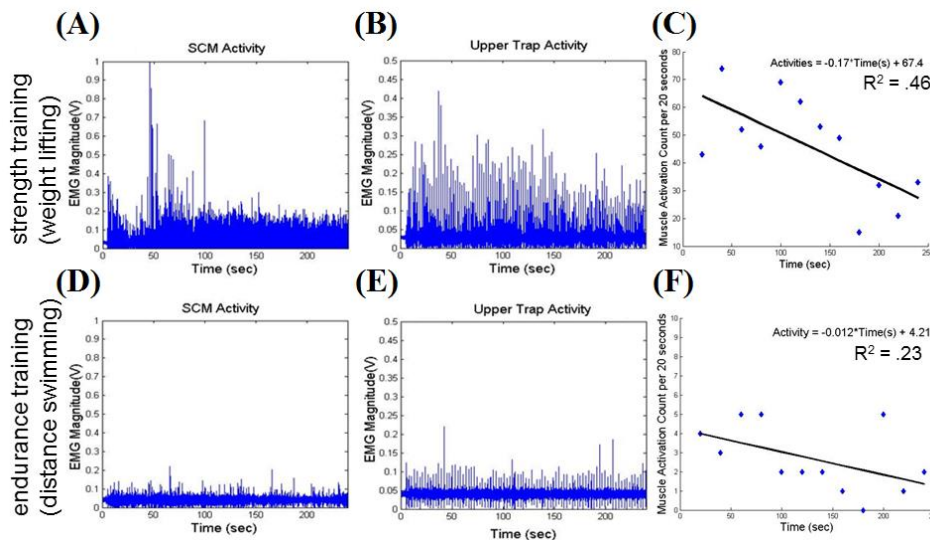


Figure 4 Muscle activities for volunteers who have regular strength training (A)-(C) vs. regular endurance training (D)-(F)

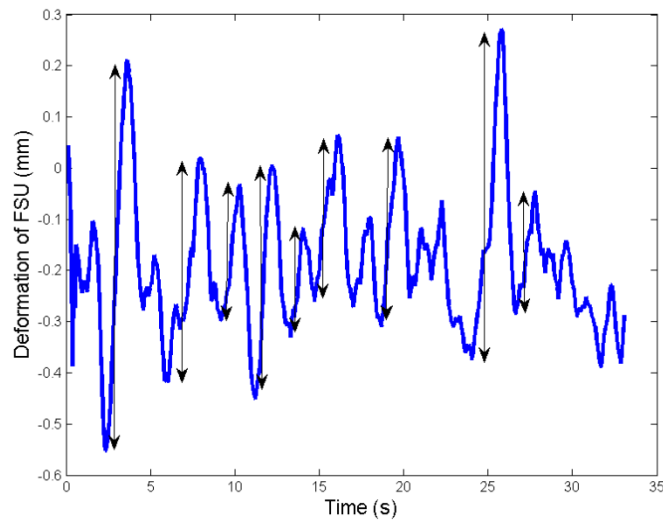


Figure 5. C4-C5 FSU compression and re-expansion during the jump tests. The amplitude of FSU motion is illustrated as double arrow.

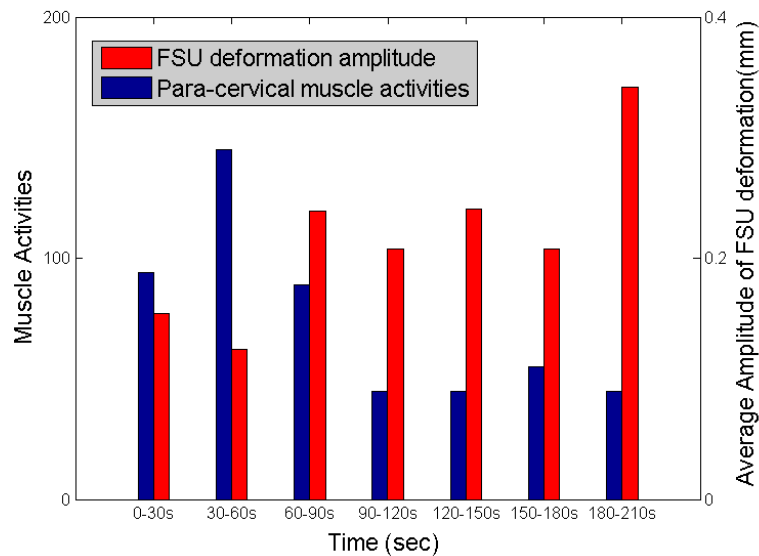


Figure 6. Integral of muscle EMG activity over 30s period compared to corresponding mean FSU deformation. Implies that initially, muscle activation stiffens FSU, manifest by attenuating IVD deformation. However, muscle fatigue diminished dampening of the load transmitted to IVD.

During jump tests, C4-C5 FSU was repetitively compressed and then recovered after each landing. Amplitude of FSU deformation, defined by the difference between minimum and maximum displacements, was shown as double arrow in Figure 5. Mean of the amplitudes (mean length of double arrows) over time, is used to characterize FSU motion levels in different time periods.

Due to muscle fatigue, para-cervical muscle activities decreased over time, when FSU deformation amplitudes gradually increased (Figure 6). The jump tests suggest that

para-cervical muscles are capable of stiffening the FSUs and minimizing the magnitude Intervertebral Disc (IVD) deformation. However, over the course of jump test, muscle fatigue was noted, and the para-cervical muscles are less capable of dampening transmitted load to IVD and deformation increases. Plotting amplitude of FSU deformation as a function of muscle activities shows an inverse correlation between FSU deformation and muscle activation (Figure 7Error! Reference source not found.).

Our preliminary data demonstrated IVD deformation inversely correlated with muscle activity, emphasizing the importance of dynamic stiffness imparted by muscle activation. Passive measurement of FSU kinetics and kinematics were not able to incorporate the muscle effect and reflect in-vivo performance during activities. Our previous study showed that a larger fraction of the compressive impulse was transmitted to the C4-C5 IVD when a subject wears a helmet compared to not wearing additional head gear when performing jumping from a height using single US. In future, we will use our current experimental data to understand the difference of kinematics and muscle dampening effect when compressive impact was applied to head between using an unweighted helmet vs. a weighted helmet.

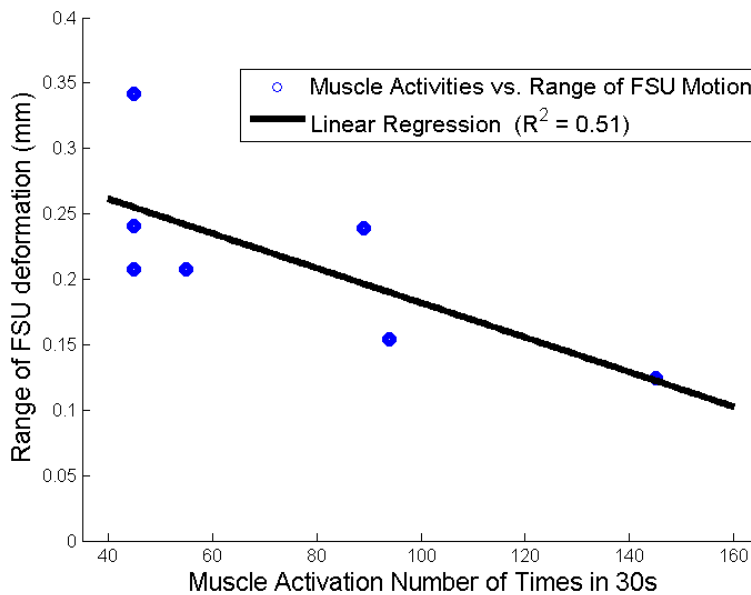


Figure 7. Amplitude of FSU deformation plotted as function of muscle activities. Linear regression showed there was an inverse correlation ($R^2=0.51$).

3.3 In-vivo US Test in Sim Environment

In order to derive a transfer function for the mechanical behavior of the cervical spine *in-vivo* in a consistent and reproducible way, we are developing a system that applies cyclic distraction/compression loads at frequencies and amplitudes that will facilitate derivation of a universal transfer function for the mechanical behavior of the

cervical spine FSUs *in-vivo* in a consistent and reproducible fashion or allow the application of different load profiles (sinusoidal, square wave, triangle, combinations thereof) that simulate the forces and moments applied to the head and neck of mounted troops during military maneuvers.

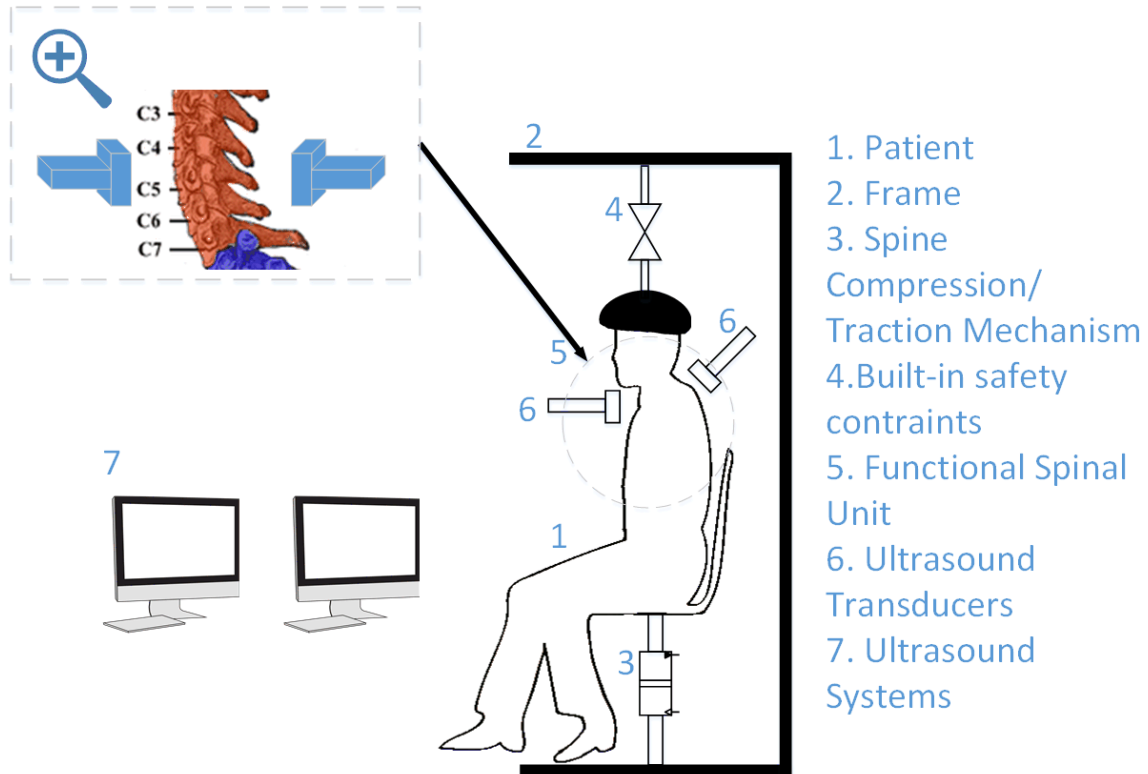


Figure 8 Schematic of cyclic load application system to head/neck of subject while sitting or standing in load frame. Under control with built-in safety constraints (4), a selected compression/traction pattern (3) is applied vertically through the seat that the subject(1) is seated, transferred up the spine to the head and neck, which is secured in a helmet rigidly fixed to an adjustable cross-bar. Simultaneously, Dual US (7) measures the deformation of selected FSU (5) in real time.

To provide controllable, safe forces to spine, the neck loading system incorporated adjustable counter-weights which tared the weight of human subject of different weights and a safety force break-away force (Figure 9). This update allowed the system to be driven by light-duty actuators as well as manual lifting. A pivot study using the system was performed to evaluate effect of voluntary neck muscle activation on C-spine properties. The actuation was done by lifting or pushing down the seat by hand. A miniature load cell on helmet was used to measure the transmitted load. The resultant deformation of C4-5 FSU was imaged by dual ultrasound system during different frequencies.

Cyclic loading at 4 different frequencies (0.5, 1, 1.5, 2Hz) were applied to the helmet of a seated human volunteer in C-spine cyclic loading system. Examination of **Error! Reference source not found.**(A) demonstrates that even though a cyclic tensile tension-compression load is applied to head, the deformation of IVD tended to be compressive only. This reflects 1) creep deformation; 2) the rate of relaxation/re-

expansion of IVD is much slower than the rate of applied external load; 3) tensile load is resisted mainly by muscles and ligaments, while the compressive load is resisted primarily by IVD. Furthermore, examination of **Error! Reference source not found.**(B) demonstrates that the volunteer contracts the para-cervical muscles, the deformation of FSU is considerably dampened.

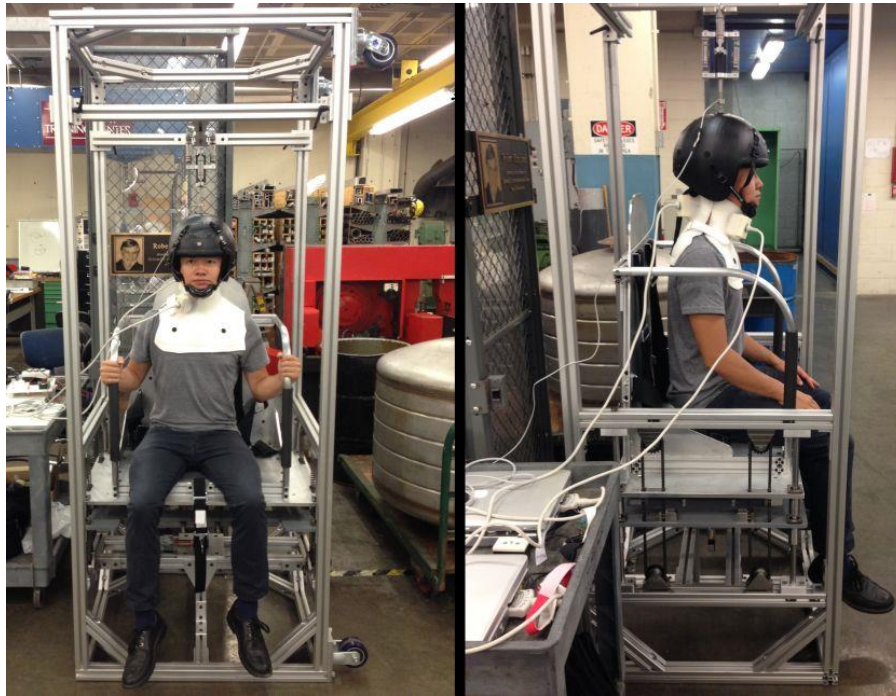


Figure 9. Modified Frame with taring weights underneath the seats, which allows seat lifting can be done by manual power. Volunteer is seated in a neutral position and wearing a cervical collar mounted with dual US at set orientation.

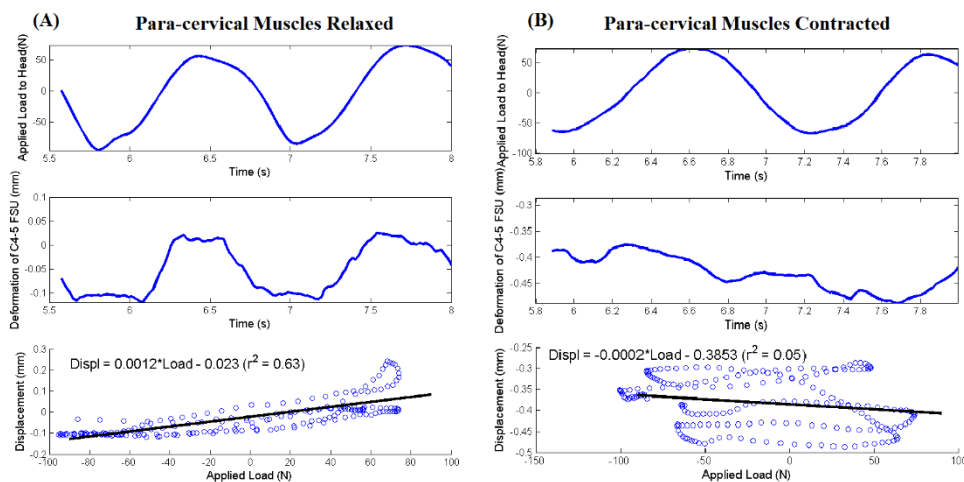


Figure 10. Representative result of dynamic testing at 1Hz. From top to bottom: 1) applied load to head over time; 2) resultant C4-C5 FSU deformation over time; 3) Displacement was plotted as a function of Applied load as a representation of the transfer function.

Together, these results support the observation from the jump tests that para-cervical muscles are capable of dampening the load applied to the IVD and that as these muscles fatigue, more load will subsequently be transferred to IVD, contributing to fatigue and “wear”. The conclusion from these tests results suggest that a combination of strength and endurance para-cervical muscles will protect our troops from cervical spine degeneration.

3.4 Fatigue Experiments on Cervical Spine Disc Segments and Developing a FE Product to Predict Spine Fatigue Using the Experimental Data.

Experiments were performed on 3 more disc segments based on the previously mentioned protocol, and a finite element model of disc with and without nucleus, which can be applied with different fatigue conditions is developed in Abaqus software. The finite element model is developed with a hyper-visco elastic material for the annulus and linear elastic materials for nucleus and end plates. The loading is applied in two steps, one single compression at 2 or 4 Hz, and second direct cyclic fatigue loading, which extrapolates the response after every 500 cycles. The direct cyclic algorithm uses a modified Newton method in conjunction with a Fourier representation of the solution and the residual vector to obtain the stabilized cyclic response directly. In direct cyclic loading the elastic stiffness serves as the Jacobian matrix throughout the analysis, the equation system is solved only once. Therefore, the direct cyclic algorithm is less expensive to use than the full Newton approach to the solution of the nonlinear equations, especially when the problem is large like in case of fatigue.

The results for 8 disc segments tested at 2Hz and 4Hz each, are compared below. The results from finite element model are also compared to the experimental data.

3.4.1 Experiments

In this set of experiments, the fatigue tests were performed on three bone disc segments, simultaneously. Two segments were tested under 150N compressive load at 2Hz and one segment was tested at 4Hz and same compressive load. The results were combined with the results of the previous segments and the average results of total 16 disc segments are presented in this report.

Magnetic resonance Image (MRI) scanning of all the disc segments was performed to ensure that there were no prior discontinuities in the spine and that the discs were representative of a healthy population. Pfirrmann scores (Pfirrmann et al. 2001) were determined from the MRI scans and all the segments with scores less than 3, determining normal to slightly diseased specimen, were selected. The posterior elements and facets of the segment were removed as per the protocol explained in the previous reports. The details of the disc segments tested are presented in Table 1.

Table 1: Details of segments tested under fatigue.

Seg. N.	PMHS	Age (Yrs)	Sex	Mass (Kg)	FSU	Initial Disc Height	Disc Area	Frequency (Hz)	Pfirrmann grades
---------	------	-----------	-----	-----------	-----	---------------------	-----------	----------------	------------------

						(mm)	(mm ²)		
1	HS-799	64	F	48.1	C6-C7	5.7366	318	2	2
2	HS-799	64	F	48.1	C4-C5	4.614	283	2	3
3	HS-799	64	F	48.1	C2-C3	5.3404	195	2	2
4	HS-798	58	M	57.6	C6-C7	6.4266	442	2	2
5	HS-795	54	M	107	C6-C7	4.5694	614	2	4
16	HS-821	59	M	106	C2-C3	5.8418	311	2	
18	HS-823	31	F	138	C4-C5	5.42	223	2	
19	HS-823	31	F	138	C6-C7	5.27	282	2	
Avg		53		80.4		5.4	333.5		
7	HS-800	58	F	79.83	C2-C3	4.5294	193	4	
8	HS-795	54	M	107	C2-C3	6.2124	325	4	2
9	HS-801	65	F	83.01	C2-C3	6.0146	227	4	2
11	HS-801	65	F	83.01	C6-C7	3.9666	627	4	
12	HS-797	67	M	99.79	C2-C3	4.4708	209	4	
13	HS-820	47	M	75	C6-C7	4.576	699	4	
14	HS-820	47	M	75	C4-C5	4.632	319	4	
17	HS-823	31	F	138	C2-C3	3.85	232	4	
Avg		54		92.6		4.8	354		

Results:

The piston stroke i.e. the displacement of the piston due to 150N load amplitude was measured for all eight segments at 2Hz and 4Hz, and the average curves are plotted in Figure 11 and Figure 12 respectively. The piston stroke was observed to decrease with increasing number of fatigue cycles. It was further reduced with increasing fatigue sets, i.e. the piston displacement for 1st fatigue set was highest and was least for 5th fatigue set, for both the frequencies. This shows that as compressive displacement of the disc decreases, the disc becomes rigid with increasing fatigue. The piston displacement was also higher at 2Hz as compared to 4Hz for all five fatigue sets, showing that at 4Hz the disc exhibits strain rate hardening effect, whereas at 2Hz the water in the disc gets enough time to move, causing more strain. The piston displacement for 5th fatigue set at 2Hz was also higher than the piston displacement for 1st fatigue set at 4Hz, showing a clear distinction between disc response at 2Hz and 4Hz. At 4Hz the piston displacement was almost constant after the first fatigue set, showing that the stiffness of the disc remained constant after the first fatigue set.

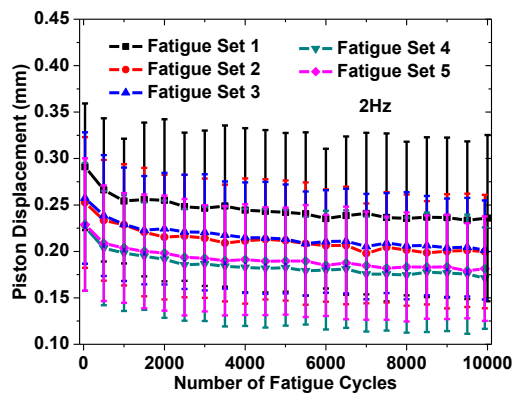


Figure 11: Average piston displacement for 5 sets at 2Hz.

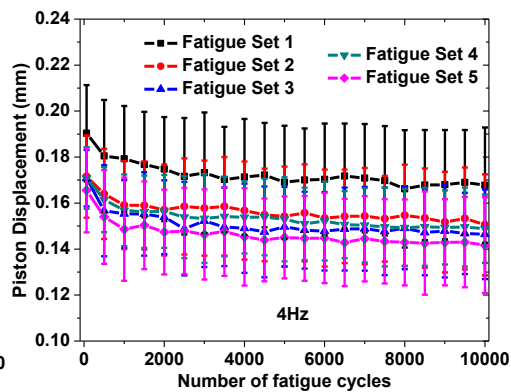


Figure 12: Average piston displacement for 5 sets at 4Hz.

Height loss due to fatigue was calculated with two sets of data. First, height loss from fatigue data was calculated as the difference between initial and final position of the piston for each fatigue set. This height loss represents the reduction in height during fatigue. Second, height loss was calculated from x ray measurements before fatigue, and after the IVD was allowed to relax post fatigue. IT represents the effective height loss, as the disc was allowed to relax post fatigue. Both height losses for all 5 fatigue sets are compared to in Figure 13 and Figure 14 for 2Hz and 4 Hz respectively. The height loss from fatigue as well as x-ray measurements are observed to be maximum during first fatigue set for both the frequencies, and was comparatively higher at 2Hz. This was again due to the strain rate hardening effect at 4Hz. The height loss calculated from x-rays was however almost the same with increase in fatigue for both the frequencies. This implies that the height loss might not necessarily dependent on frequency, but it depends on the number of cycles and magnitude of loading. From this it can be concluded that relaxation time for a person exposed at 2Hz and 4Hz fatigue loading could be same.

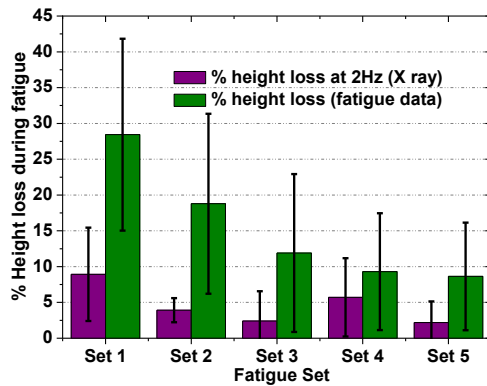


Figure 13: Height loss for 5 sets at 2Hz.

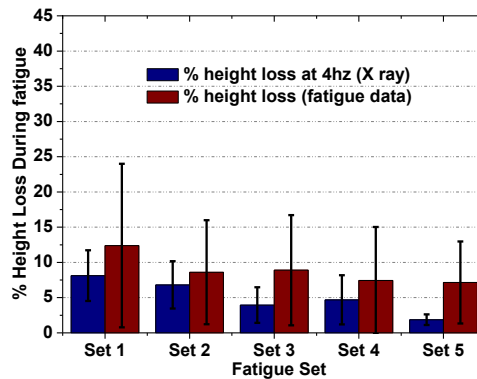


Figure 14: Height loss for 5 sets at 4Hz.

The stiffness of the IVD was calculated as the ratio of force to displacement for every cycle. From Figure 15 the stiffness of the discs tested at 2Hz can be observed to increase with fatigue. The stiffness for 2nd and 3rd fatigue set was higher than 1st fatigue set and the behavior was almost identical. Whereas the 4th and 5th fatigue sets show even stiffer and identical behavior. For the segment tested at 4Hz it can be observed from Figure 16 that the stiffness increased after the 1st fatigue set and was almost constant for remaining four fatigue set, suggesting some damage in terms of discharge of fluid in nucleus and steady material properties after the 1st fatigue set. It still needs to be verified with some imaging technique. The overall stiffness of the segments tested at 4Hz was higher as compared to the segments tested at 2Hz.

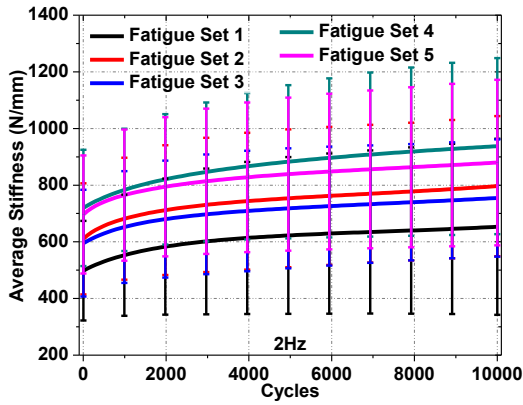


Figure 15: Average stiffness for 5 sets at 2Hz.

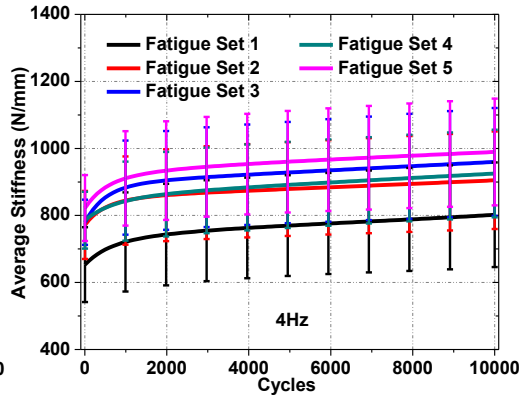


Figure 16: Average stiffness for 5 sets at 4Hz.

In Figure 17 and Figure 18 average of stress versus strain plots from the static compression tests of all five segments are shown. The stiffness of the segments fatigued at 2 Hz was similar post first two fatigue sets. The stiffness increased further for the next three fatigue sets. This shows that at 2Hz the disc is palpated during the first two fatigue sets and, during the 3rd, 4th and 5th fatigue sets there is loss in viscoelasticity and thus increase in stiffness. The disc segments fatigued at 4 Hz showed constant stiff behavior after the first fatigue set. Suggesting that viscoelasticity loss is maximum during the first fatigue set and if there is a damage, it will be initiated during the first fatigue itself. The increase in stiffness of segments was almost similar for both the frequencies, though the height loss in segments tested at 4Hz is not as much.

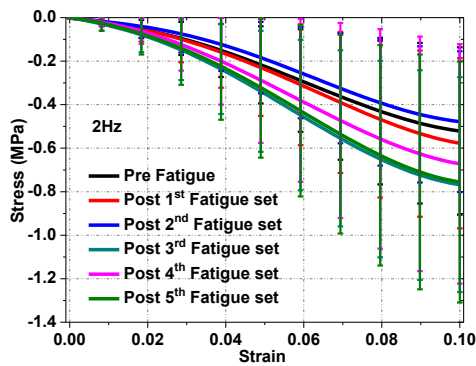


Figure 17: Stress Strain plots for static compression test pre and post 5 fatigue sets (2Hz).

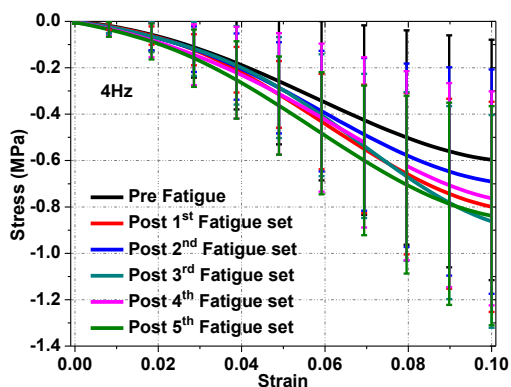


Figure 18: Stress Strain plots for static compression test pre and post 5 fatigue sets (4Hz).

In the viscoelastic tests 10% strain was applied to the disc and the stress was allowed to relax for 30 min. The stress relaxation curves from the viscoelastic tests for segments tested at 2Hz and 4Hz are plotted in Figure 19 and Figure 20 respectively. The viscoelastic properties of the discs fatigued at 2Hz did not change a lot for first two fatigue tests, whereas the initial and final stiffness increased, and the toe region of the stress relaxation curve shifted to the right post 3rd, 4th, and 5th fatigue sets, suggesting

loss in viscosity. The viscoelastic response offered for 10% strain by the segments tested at 4Hz was almost similar after the first fatigue test, similar to that observed from piston displacement, stiffness and static compression plots. The viscoelastic material parameters for average viscoelastic curves, pre and post fatigue are tabulated in Table 2.

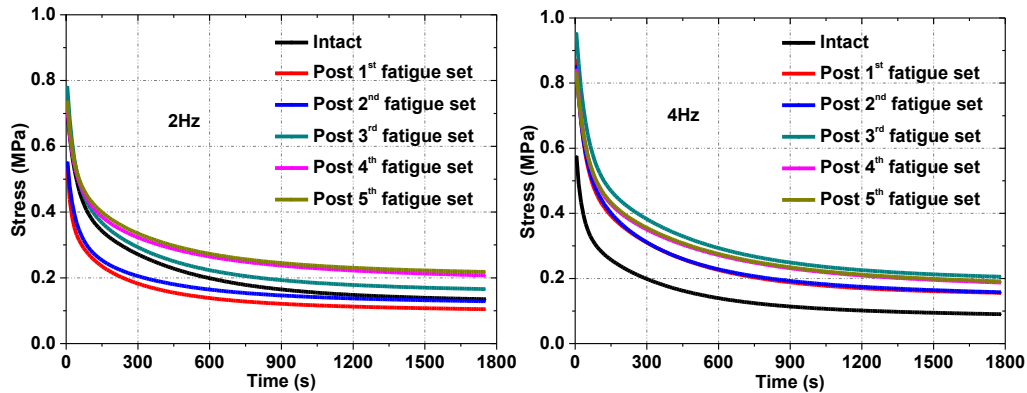


Figure 19: Average stress relaxation curve pre and post 5 fatigue sets (2hz). Figure 20: Stress Strain plots for static compression test pre and post 5 fatigue sets (4hz).

Table 2: Average quasi linear viscoelastic material parameters

Parameters	A	B	a	b	c	d	g	h
2Hz								
Intact	0.0032	1.2497	0.3320	0.0245	0.2998	0.0025	0.1613	5.5E-5
Post 1 st Fatigue	0.0009	1.4965	0.2744	0.0342	0.2525	0.0033	0.1708	8.0E-5
Post 2 nd Fatigue	0.0007	1.5625	0.2858	0.0543	0.2999	0.0037	0.2354	3.3E-5
Post 3 rd Fatigue	0.0093	0.9119	0.3188	0.0287	0.3438	0.0029	0.2008	4.4E-5
Post 4 th Fatigue	0.0096	1.0099	0.3185	0.0210	0.2755	0.0025	0.2982	6.3E-5
Post 5 th Fatigue	0.0103	0.9518	0.2770	0.0202	0.2654	0.0026	0.2895	7.8E-5
4Hz								
Intact	0.0033	1.2065	0.3070	0.0380	0.2841	0.0034	0.1026	6.8E-5
Post 1 st Fatigue	0.0064	1.0749	0.2954	0.0310	0.2156	0.0028	0.1073	8.1E-5
Post 2 nd Fatigue	0.0045	1.1182	0.2321	0.0457	0.3156	0.0037	0.1289	6.8E-5
Post 3 rd Fatigue	0.0055	1.1620	0.4002	0.0172	0.2151	0.0019	0.1683	7.3E-5
Post 4 th Fatigue	0.0048	1.2257	0.3458	0.0233	0.2979	0.0022	0.1668	6.6E-5
Post 5 th Fatigue	0.0086	0.9625	0.3414	0.0238	0.2729	0.0024	0.2033	7.4E-5

Summary:

In this report experimental results, for 16 segments fatigued at 150N compressive force at 2Hz and 4Hz loading frequencies, for 5 sets of 10,000 cycles are reported. Static tension-compression and viscoelastic stress relaxation tests were performed before the first and after each fatigue set. Average results for the segments tested at 4Hz showed strain rate hardening effect and thus were not strained as much as discs tested at 2Hz.

The piston displacement and the disc height loss, was maximum during the first 10,000 cycle fatigue set for both the frequencies. As the number of cycles increased, the IVD

demonstrated a decreasing piston displacement for segments tested at 2 Hz, whereas for the segments tested at 4 Hz the piston displacement was almost identical for last four fatigue sets. After first fatigue set the strain in all the sets at 4 Hz was almost identical suggesting some damage, which needs to be further investigated using imaging. However the effective height loss from xrays, measured between two fatigue sets was observed to be similar for segments tested at 2Hz and 4 Hz.

3.4.2 Finite Element Modeling

In the previous deliverable, a finite element model with homogeneous disc and end plates was developed in the Abaqus software and the fatigue load was applied in two steps:(1) a uniform load of 150N at 2Hz was applied to the superior end plate. , The boundary condition at the inferior endplate was fixed in all degrees-of-freedom. (2) a direct cyclic step simulating 10000 compression cycles based on the previous step history. To start with the disc was modeled with a homogenous hyper visco-elastic material termed as 'model A' below. The model A performed well for the prescribed boundary condition. So to accommodate more realistic response, the model A was further improved with nucleus at the center, as a linear elastic material and is called 'model B' below.

The finite element model was developed from a CT scan (Figure 21) of a 50th percentile male (25 years, 78 kg total body mass, and 183 cm stature). The model contained, 676 quadratic shell elements and 845 hexahedral solid elements. The disc was modeled as hyper visco-elastic material, with properties of the disc without fatigue obtained from the static compression test and viscoelastic stress relaxation. The end plates were modeled with a linear elastic material. In model B, the nucleus (35% of total volume of disc) was modeled with a linear elastic material (Panzer 2006).

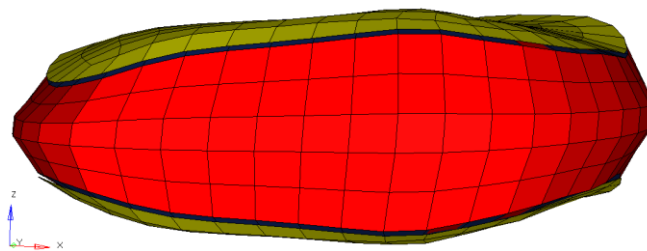


Figure 21: Developed disc FE model.

Boundary Conditions:

A cyclic load at 2Hz or 4Hz frequency as in experiments was applied to the developed FE model of the disc. As per experiments, cyclic load was applied to the disc segment as shown in Figure 22, all the surface nodes of the inferior end plate were constrained in x, y and z direction and a cyclic load of 150N was applied in z direction on the superior end plate. For 2 Hz test reconstruction one cyclic simulation was performed as step 1. The next step of computation is the direct cyclic loading in which 10000 fatigue cycles are applied.

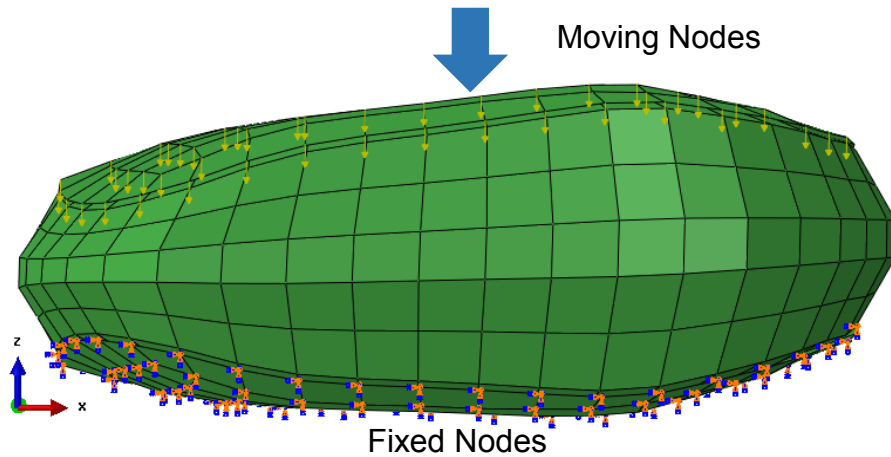


Figure 22: Boundary Conditions (disc segment)

Results:

Model A: Model A took about 1 Hour, on 64GB ram and 8 core processor, for 2 Hz fatigue simulation. Figure 23 shows the Von Mises stress distribution in the disc at the end of the step 2, i.e., 10000 cycles. The magnitude of the residual stress was present in the lateral parts of the disc. The displacement of the nodes during 10,000 cycles was compared to the piston stroke from experiments for the first 10,000 cycles (Figure 24). The experimental stroke and nodal displacements were comparable. The stroke was maximum during the first 1000 cycles, followed by a plateau showing the effect of viscoelastic properties in this first 1000 cycle period.

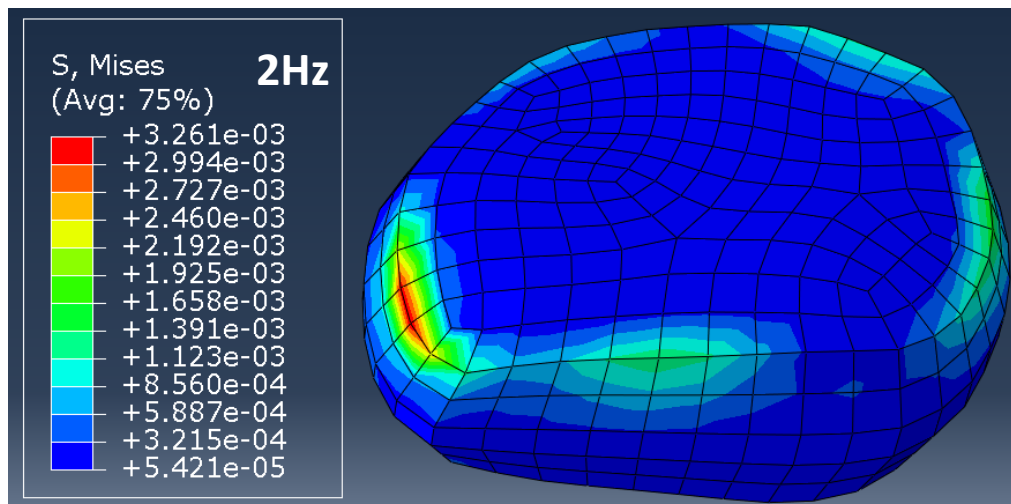


Figure 23: Von Misses (residual) stress (MPa) distribution post fatigue (2hz)

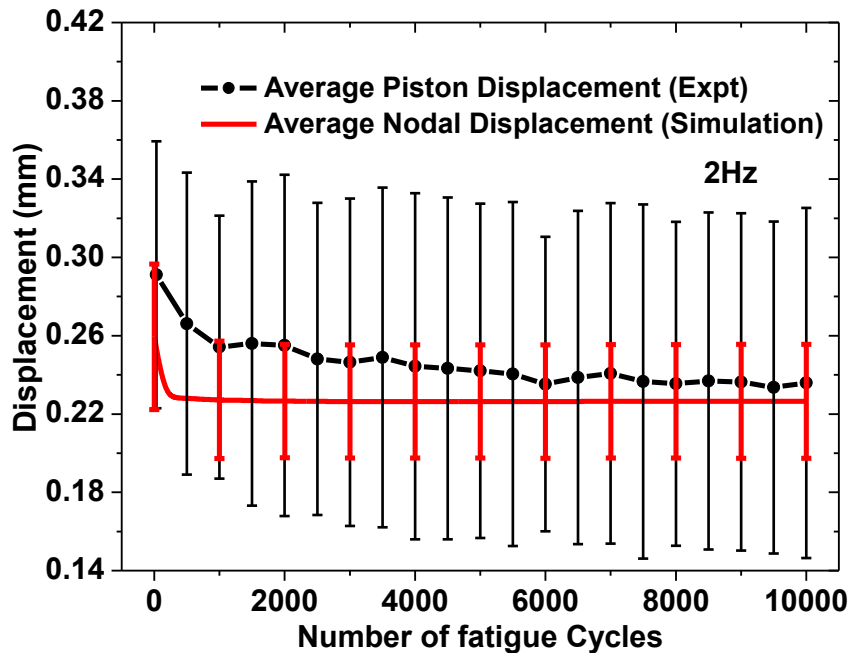


Figure 24: Comparison of piston stroke from experiments to the nodal displacements

The FE model was then subjected to 4 Hz compressive load of 10,000 cycle. The nodal displacements were lesser for 4Hz than at 2 Hz, demonstrating strain rate hardening in the intervertebral disc. The average displacements of all the nodes from simulations at 2 Hz and 4 Hz are plotted in Figure 25. The nodal displacements at 4hz had discrepancy with the experimental stroke at 4Hz, which can be attributed to the assumptions in the hyper elastic material model formulation in the Abaqus software.

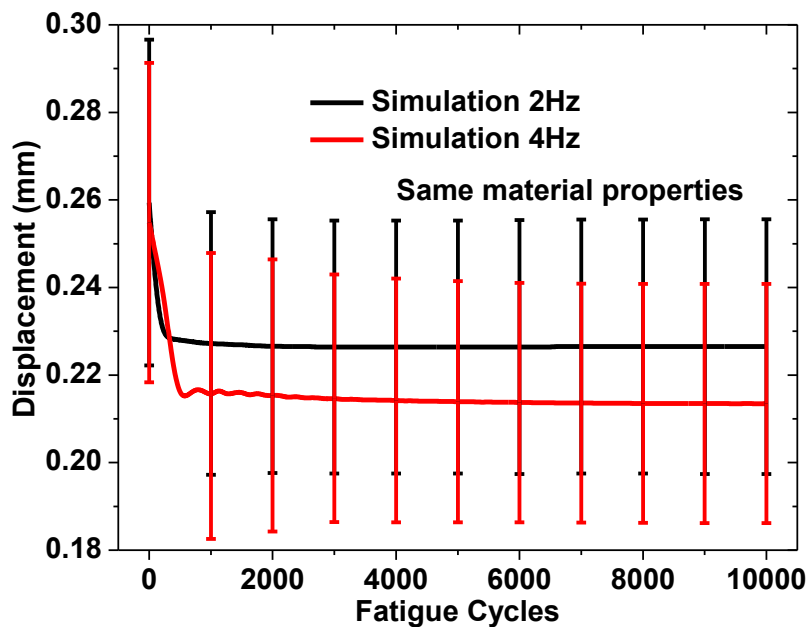


Figure 25: Comparison of nodal displacements at 2hz and 4hz

It can be observed from the experimental data (Figure 15 and Figure 16) that the initial stiffness of the segments tested at 4 Hz is approximately 1.5 times the stiffness of the segments tested at 2 Hz. Assuming that the stiffness of the segment to also increase in the same ratio at 4Hz, the results for simulation at 4 Hz are shown in Figure 26. The piston stroke and nodal displacement from simulation are in good agreement at this frequency.

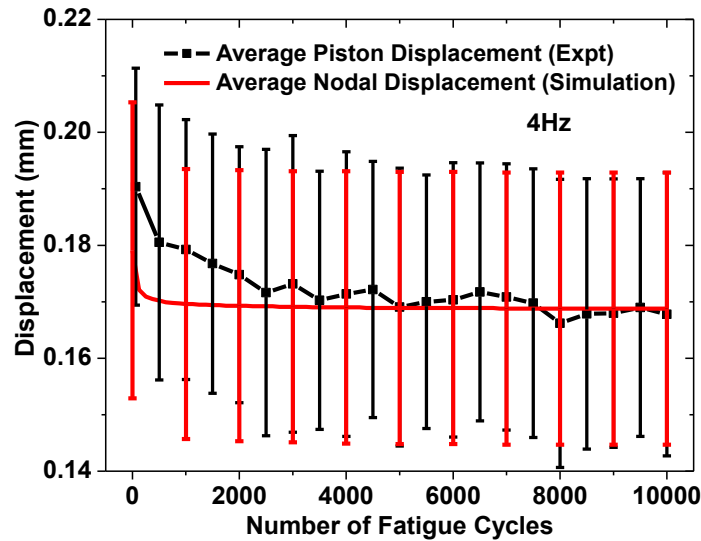


Figure 26: Comparison of piston stroke from experiments to the nodal displacements

Figure 27 shows the residual Von misses after 10,000 fatigue cycles at 4 Hz. The location of stress distribution was similar to 2 Hz, however the magnitude residual stress was greater. This suggests that stress and applied frequency are positively correlated.

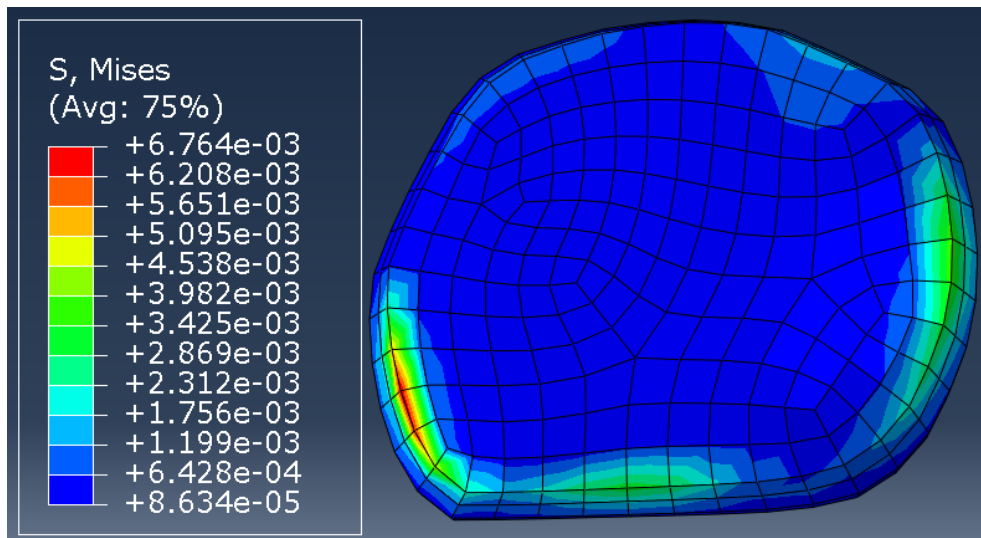


Figure 27: Von Misses (residual) stress (MPa) distribution post fatigue (4hz)

Model B: Following the encouraging findings from the model A, in this subsequent model B, the center of the disc was modeled with an incompressible elastic material simulating more accurately its in vivo nature. The nucleus was assumed to occupy 35%

by volume of the disc and was modeled with material properties from Jones and Wilcox 2008 .

The model was subjected to similar boundary conditions and the simulation took almost same time, of about 1 hour on 8 core and 64 GB ram machine. The simulations were carried out at 2 Hz and 4 Hz as in the experiments and the displacement of the nodes were compared to piston displacements. A combined corridor for experimental piston displacement for both 2Hz and 4Hz frequencies, and the simulation nodal displacements are plotted in Figure 28. The nodal displacements from the both the frequencies fit well within the experimental corridor, indicating the improvement in the modeling process.

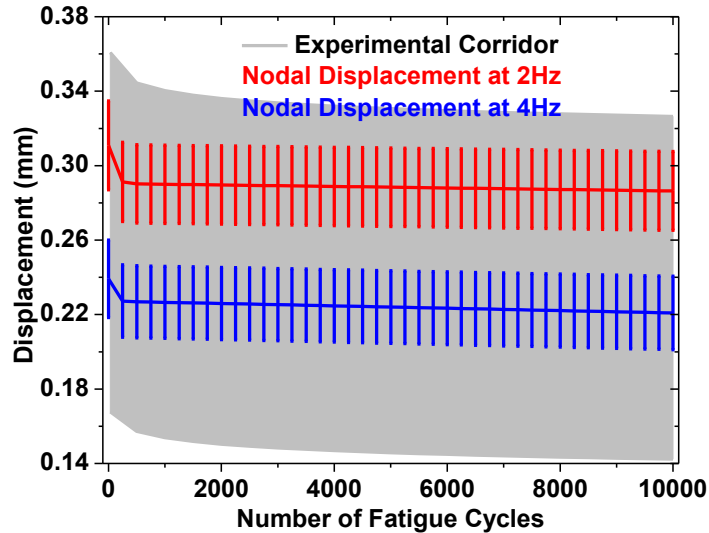


Figure 28: Comparison of piston stroke from experiments to the nodal displacements at 2Hz and 4Hz

The residual von mises stress, principal stresses in x, y and z directions and pressure from fatigue were compared for the two simulations (i.e. 2Hz and 4Hz). From the pressure it was observed that, nucleus was under maximum pressure and it reduced radially in the annulus. The maximum residual stress in the annulus occurred in the lateral direction, while the nucleus was under the least stress. The principal stresses in the superior-inferior direction showed that both the annulus and nucleus were under similar magnitudes, reflecting the applied load vector. From the Von mises stress it was observed that nucleus and annulus in the lateral directions was under maximum stress. The contour plots for both the frequencies for pressure, principal stresses and Von mises stresses are shown in Figure 29 and Figure 30 below.

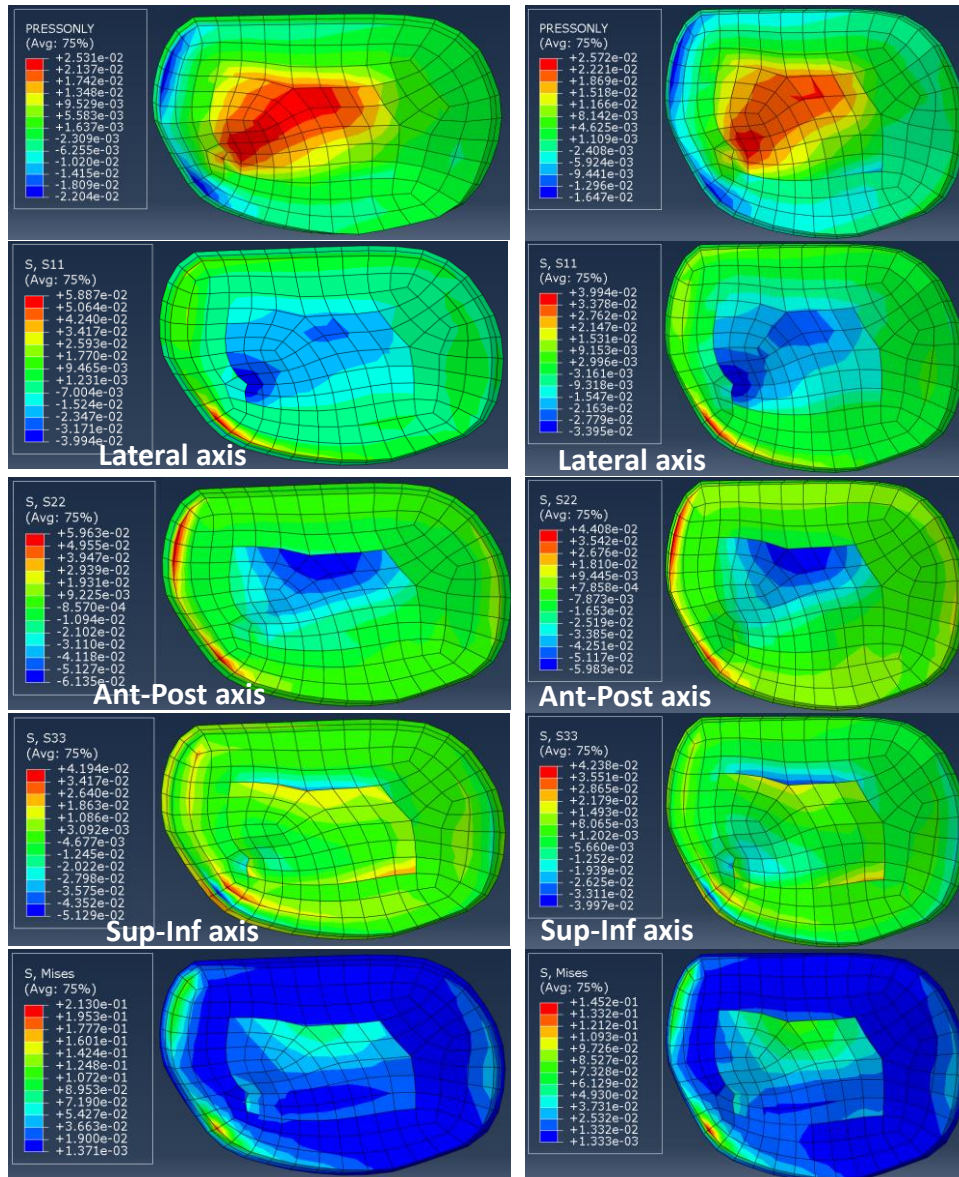


Figure 29: Contour plots for residual pressure, principal stress, and von mises stress for disc at 2Hz

Figure 30: Contour plots for residual pressure, principal stress, and von mises stress for disc at 2Hz

Summary:

In this quarter, FE model of the inter vertebral disc without nucleus (model A) and with nucleus (model B) was developed in Abaqus software. The boundary conditions and material properties are adopted in the model from experimental data and literature. Model A showed good correlation to the experimental data. Model B with separations in its two components (i.e. the annulus and the nucleus) demonstrated differences in regional stress distributions during the fatigue loading process. At 4Hz, the model was

stiffer than at 2 Hz, a phenomenon which validated the experimental observations. The peak principal stress distributions in superior-inferior direction was on the superior regions in the simulation at 4 HZ, although the nodal displacements were not the greatest along the same direction. This demonstrates that with increasing frequency, there may be regional stress accumulations on the rostral side of the disc, with lesser transmission to the inferior region. These results suggest that a higher frequency of loading may be more injurious due to fatigue loading

In future quarters parametric analysis will be performed on the disc model based on volume on nucleus. Geometry of the disc and position of the nucleus can influence the results and efforts will be made to understand the injury mechanics.

4. CONCLUSION

We have developed a dual ultrasound system can be used to non-invasively measure IVD deformation and mechanical compliance *ex-vivo*, and provide real-time images of IVDs and dynamic vertebral motion *in-vivo* during simulated tasks relevant to acute and chronic cervical spine injury and disease. Software was developed to track the motion of a user-specified region of interest that corresponds to the anterior and posterior bony profiles of cervical vertebrae. For motion frequencies up to 8Hz, US accounted for 95% of the true IVD displacements and the estimated error was 0.06mm. In our preliminary experiments using the dual US system *ex-vivo and in-vivo*, we studied the dependence of the compliance of IVD measured directly vs. the subjects' age and Pfirrmann Grade measured by MRI. The "quality" and hydration of the IVD affected the measured compliance, while the damping coefficient was unaffected. The IVD/FSU for younger specimen/subject tends to be more compliant in creep test analysis compared to older specimen/subject. we show voluntary para-cervical muscle activities affects the dynamic FSU stiffness and deformation of IVD during repetitive tasks. The jump tests suggest that para-cervical muscles are capable of stiffening the FSUs and minimizing the magnitude IVD deformation. However, over the course of jump test, muscle fatigue was noted, and the para-cervical muscles are less capable of dampening transmitted load to IVD and deformation increases. The result that volunteer who has strength training experience faster neck muscle fatigue suggests proper training of neck may lead to prevention of neck injuries for laborers working in dynamic environment. To achieve more reliable measurement of IVD properties *in-vivo*, a diagnostic system was developed that safely applies dynamic cyclic loads to cervical spine over a range of programmable frequencies and amplitudes that simulate operational conditions.

In C-spine modeling, it was observed that the experimental conditions during fatigue testing affect outcomes drastically; soft tissues become dehydrated quickly under ambient conditions that are ameliorated by using a saline bath. The results from C-spine cyclic loading were used to generate material parameters which were incorporated into the FE model for IVD fatigue. Matlab algorithms were developed to discretize the FE model of the IVD so that changes in the material properties of the nucleus and annulus elements as a function of number of applied load cycles were updated during the fatigue test FE analysis to reflect progressive deterioration of their material properties obtained from the fatigue experiments.

5. REPORTABLE OUTCOMES

5.1 Conference Presentation

Ultrasound Can Measure Dynamic Motion of Cervical Spine Intervertebral Disc, Orthopaedics Research Society 2013 (Poster)

Clinical Ultrasound Can Measure Dynamic Intervertebral Disc Deformation In-vivo, Orthopaedics Research Society 2013 (Poster)

Real-Time Ultrasound Can Measure Dynamic Properties of Cervical Spine Intervertebral Disc,

Orthopaedics Research Society 2014 (Conference Poster)

3D Kinematics Using Dual Ultrasound Stereographic Imaging of Human Cervical Spine, Aerospace Medical Association (Conference Oral Presentation)

Ultrasound Imaging of Cervical Spine Intervertebral Discs, 2014 World Congress of Biomechanics

Use of Portable Ultrasound to Measure Dynamic Motion of Cervical Spine Ex-Vivo and In-Vivo, Biomedical Engineering Society 2014 (Conference Oral Presentation)

Dual Ultrasound Can Measure Kinematic Motion and Intervertebral Disc Deformation of Cervical Spine, Orthopaedics Research Society 2015 (accepted as Conference Poster)

Dynamic Ultrasound Imaging of Cervical Spine Intervertebral Discs, 2013 IEEE International Ultrasonics Symposium (Poster)

Dynamic Ultrasound Imaging of Cervical Spine Intervertebral Discs, 2014 IEEE International Ultrasonics Symposium (Conference Oral Presentation)

Muscle Fatigue Affects Functional Spinal Units Deformation Measured by Dual Ultrasound, Orthopaedics Research Society 2016 (Conference Poster)

5.2 Publication

Zheng M, Shiuan K, Masoudi A, Buckland D, Szabo T, Snyder B: Dynamic ultrasound imaging of cervical spine intervertebral discs, Ultrasonics Symposium (IUS), 2013 IEEE International, Page(s): 836-839

Zheng M, Masoudi A, Buckland D, Stemper B, Yoganandan N, Szabo T, Snyder B: Dynamic ultrasound imaging of cervical spine intervertebral discs, Ultrasonics Symposium (IUS), 2014 IEEE International, Page(s): 448-451

Umale S, Stemper BD, Zheng M, Masoudi A, Fama D, Yoganandan N, Snyder BD. Methodology to calibrate disc degeneration in the cervical spine during cyclic fatigue loading. Biomed Sci Instrum (in review).

Umale S, Stemper BD, Zheng M, Masoudi A, Fama D, Yoganandan N, Snyder B: Progressive changes in cervical spine intervertebral disc properties during cyclic compressive fatigue loading. ASME Summer Biomechanics, Bioengineering, and Biotransport Conference, Snowbird Resort, Utah, June 17-20, 2015 (in review).

Umale S, Stemper BD, Zheng M, Masoudi A, Yoganandan N, Snyder BD. Changes in cervical intervertebral disc viscoelasticity during repetitive axial loading: A preliminary report. 2015 Annual Meeting of the Orthopedic Research Society, Las Vegas, NV, March 28-31, 2015.

6. REFERENCE

Rahimi A, Morency L-P. 2001. "Reducing drift in parametric motion tracking." *Computer Vision, 2001. ICCV 2001. Proceedings. Eighth IEEE International Conference on.* Vol. 1. IEEE, Abramowitch, Steven D. 2004. "An Improved Method to Analyze the Stress Relaxation of Ligaments Following a Finite Ramp Time Based on the Quasi-Linear Viscoelastic Theory." *Journal of Biomechanical Engineering* 126 (1): 92.

Qasim, Muhammad, Raghu N. Natarajan, Howard S. An, and Gunnar B.J. Andersson. 2012. "Initiation and Progression of Mechanical Damage in the Intervertebral Disc under Cyclic Loading Using Continuum Damage Mechanics Methodology: A Finite Element Study." *Journal of Biomechanics* 45 (11): 1934–40.

Qasim, Muhammad, Raghu N. Natarajan, Howard S. An, and Gunnar B.J. Andersson. 2014. "Damage Accumulation Location under Cyclic Loading in the Lumbar Disc Shifts from Inner Annulus Lamellae to Peripheral Annulus with Increasing Disc Degeneration." *Journal of Biomechanics* 47 (1): 24–31..

Stemper, Brian D., Jamie L. Baisden, Narayan Yoganandan, Barry S. Shender, and Dennis J. Maiman. 2014. "Mechanical Yield of the Lumbar Annulus: A Possible Contributor to Instability: Laboratory Investigation." *Journal of Neurosurgery: Spine* 21 (4): 608–13.

Toms, Stephanie R., Greg J. Dakin, Jack E. Lemons, and Alan W. Eberhardt. 2002. "Quasi-Linear Viscoelastic Behavior of the Human Periodontal Ligament." *Journal of Biomechanics* 35 (10): 1411–15.

Wheeldon, John A., Frank A. Pintar, Stephanie Knowles, and Narayan Yoganandan. 2006. "Experimental Flexion/extension Data Corridors for Validation of Finite Element Models of the Young, Normal Cervical Spine." *Journal of Biomechanics* 39 (2): 375–80.

